Low Temperature Plasma Technology Laboratory
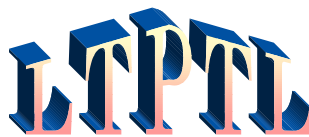
**Evidence for Trivelpiece-Gould modes
in a helicon discharge**

D.D. Blackwell, T.G. Madziwa, D. Arnush, and F.F. Chen

Electrical Engineering Department, UCLA

LTP-106   June, 2001

LTPTL

Electrical Engineering Department
Los Angeles, California 90095-1594

UNIVERSITY OF CALIFORNIA • LOS ANGELES

Evidence for Trivelpiece-Gould modes in a helicon discharge

D.D. Blackwell, T.G. Madziwa, D. Arnush, and F.F. Chen

Electrical Engineering Department, University of California, Los Angeles, California 90095-1594

The high ionization efficiency of helicon discharges has been attributed to either Landau damping or mode coupling to Trivelpiece-Gould (TG) modes. To support the latter mechanism, TG modes were detected directly by measuring their radiofrequency current with a J-dot probe, thus elucidating the physical mechanism of these enigmatic plasma sources

Helicon (H) discharges, in which radiofrequency (rf) energy is absorbed by bounded whistler waves, have been studied intensively because of their ability to generate high plasma densities at low pressures and RF powers, with applications to semiconductor processing and space propulsion. Shamrai et al.[1] have proposed that the efficiency of the absorption mechanism is not due to Landau damping, as hypothesized by Chen[2], but to coupling to Trivelpiece-Gould (electron cyclotron) modes, which, being quasi-electrostatic, are rapidly absorbed as they propagate inward from the radial boundary. Computations by Borg and Boswell[3] and by Arnush[4] have verified that this mechanism gives plasma loading resistances in agreement with experiment[5], but direct detection of TG modes is difficult because these modes tend to be localized in an irresolvably thin layer near the surface. However, at magnetic fields below about 50G, TG modes extend far into the interior of the discharge, and their effect on the wave shapes should be detectable.

Experiments were done in the 10 cm diam, 110 cm long device shown in Fig. 1. To facilitate comparison with theory, the simplest antenna was used: an azimuthally symmetric ($m = 0$) loop, shown in Fig. 2a. A Faraday shield (Fig. 2a) was used to minimize capacitive coupling, which could cause plasma asymmetries[6]. Diagnostics included Langmuir probes, magnetic ("B-dot") probes for B_z and B_θ of the wave, and a new rf current probe, to be described later. The antenna was located 15 cm from a conducting endplate and 30 cm from the midplane port, where most of the data were taken. The discharge was operated in 2–3 mTorr of argon with $0.8 - 1$ kW of 11 MHz power and a dc field $\mathbf{B}_0\hat{\mathbf{z}}$ of 25-60G. This range of parameters gave stable discharges of density $n = 2 - 10 \times 10^{11}$ cm^{-3} in which the TG mode was predicted[7] to have similar radial wavelengths and thus be detectable. This narrow window is illustrated in the dispersion relation of Fig. 3 for coupled H-TG modes[7] at a density of 4×10^{11} cm^{-3}. At a given k, such as that shown by the dotted line, the two values of β corresponding to the H and TG modes are close only for a small range of B_0 around 30G. At fields as high as 300G, β_{TG} would be so large that the TG mode would be confined to a thin edge region. Initial measurements of $|B_z|$ showed little evidence, however, of the H-wave profile caused by the presence of a TG mode. This effect could be amplified, however, by measuring the rf current J_z rather than the rf magnetic field B_z.

That J_z is more sensitive to the TG mode than B_z can be seen from simple helicon theory. Both the H and TG waves satisfy[7]

$$\mu_0 \mathbf{J} = \nabla \times \mathbf{B} = \beta \mathbf{B}, \qquad J_z = (\beta / \mu_0) B_z, \tag{1}$$

where

$$\beta_{TG,H} = \frac{k}{2\delta}\left(1 \pm \sqrt{1 - \frac{4k^2\delta^2}{k_s^2}}\right), \tag{2}$$

$\delta = \omega / \omega_c$, $k_s = \omega_p / c$, and k is the axial wavenumber. Here β_{TG} is the upper (+) root, and β_H the lower (−) root, so that their ratio is always >1 (*cf*. Fig. 3). Eq. (1) indicates that if both modes have the same $|B_z|$, the TG mode will have larger $|J_z|$ by the ratio β_{TG}/β_H. This is evident in the theoretical profiles shown in Fig. 4a as well as the measured profiles of Figs. 4b and 4c, where the outer peak due to the TG mode can be seen only in $|J_z|$.

To measure J_z, a miniature J-probe (essentially an RF Rogowski coil) was made and carefully calibrated. The probe consists of 150 turns of coated wire wound poloidally on an insulating coil form, resulting in a ring of ~4 mm i.d. and ~9 mm o.d. To cancel the toroidal component of the coil current, a return loop was wound in a groove on the inside, as shown in Fig. 2b. The windings were covered with a copper Faraday shield with a toroidal slit. The coil was mounted on a 3.2-mm o.d. stainless steel tube, and the twisted-pair leads were threaded through an inner shield consisting of an 0.8-mm diam hypodermic needle. The leads were connected to a 1 − 1 balun transformer, and the unbalanced signal then passed through a bandpass filter to a digital oscilloscope. The probe was deployed in the port 30 cm downstream from the antenna (Fig. 1). The sensitivity of the probe was measured by passing a known rf current in a wire along the major axis of the torus. Rejection of electrostatic signals was tested by immersing the coil in a mercury bath and applying a known rf voltage to the mercury. The pickup per volt applied was 0.4 mV, compared with a typical J_z signal of 10-30 mV. The most difficult task was to eliminate the B-dot signal from B_z fields passing through the torus and imperfectly canceled by the return loop described above. This effect was checked by placing the coil in a Helmholtz coil which produced a known B_z field. The pickup from a 1-G B_z field at 11 MHz was only 0.2mV. These sources of error added to <10%. Finally, the J-probe was tested inside the pulsed helicon discharge. Rotating the probe 180° gave a reversed signal to within 10°. Rotating it 90° yielded J_θ instead of J_z, with a completely different radial profile, as shown in Fig. 5. Withdrawing the probe into the port arm dropped the signal by 90%. B_z pickup was tested by plugging the opening in the J-probe with a ceramic disk. The signal was reduced by only a factor of 2–4; this was attributed to displacement current through the ceramic. Of 20 coils constructed, only two passed all these tests.

Inserting the probe through the center of the plasma necessarily disturbs the discharge. Hence, in the graphs shown, data on both sides of the axis were averaged to produce a symmetric pattern to compare with theory. Data could be reproduced from month to month. The theoretical curves were computed with the codes developed by Arnush[4,8], incorporating H–TG mode coupling; electron collisions with neutrals and ions at $T_e = 3$ eV and $p = 3$ mTorr; the radial density gradient; and antenna coupling, including the effects of image currents on the endplate. For a radially uniform density, the Shamrai Bessel function solutions[1] are used, whereas for non-uniform density differential equations are solved, and the H and TG modes are distinguished by their behavior near the axis[8]. Instrumental resolution was included by averaging the curves over the i.d. of the J-probe. The computations were for an infinitely long plasma with no axial gradients. Tests were made of the effect of the conducting endplate near the antenna. Imposing the boundary condition $J_z = 0$ at the endplate

had a noticeable affect on the J_z profiles but did not change their general character. The boundary condition $\mathbf{E}_\perp = 0$ gave less reasonable results. Ignoring reflections from the ends gave the best agreement.

Preliminary measurements given elsewhere[9] verified that the discharge was operating in the normal helicon regime. Profiles of wave B_z and B_θ at 100G and above exhibited the classical Bessel function shape of simple H waves[10]. That these $m = 0$ profiles were symmetric was checked with two probes 90° apart in azimuth; this was not the case with $m = 1$ waves generated by a helical antenna, presumably because of the difficulty in constructing a helical Faraday shield of sufficient accuracy. Phase measurements of B_z along the axis showed propagation with an axial wavelength agreeing with theory. Figure 4c shows a typical density profile, which is uniform except for a small rolloff at the edge. The electron temperature is ~3eV; it affects only the collisional term in the computations.

Figure 6 shows the $|J_z|$ profiles at 30G and three densities, as compared with curves calculated with the HELIC code with and without the TG mode included. With collisions, there can be no solution with $E_z = 0$ representing the simple H mode; the "no TG" curve is the component that behaves like a Bessel function near the axis. In each case, it is seen that the data show the "wings" due to the presence of the TG mode which are not present with the H mode alone. The J-probe is unable to resolve the fine structure of these wings, but they are clearly present. The magnitudes and positions of the TG peaks could not always be reproduced by the theory, partly because of equilibrium profile effects not included in the calculations, and partly because of imperfections in the J-probe, as explained in the calibration procedures. In some cases adjusting the density in the computation improved the fit. This is reasonable because a) the density at the probe port can differ from that under the antenna, depending on the location of the downstream density peak[11], and b) densities found from saturation ion currents can be in error by as much as 100%[12]. Note that at $n = 6.9 \times 10^{11}$ cm^{-3} destructive interference between the H and TG modes has suppressed the TG wings; this effect is seen in both the data and the theory. Figure 7 shows the $|J_z|$ profiles for 30, 40, and 50G at $n = 4.2 \times 10^{11}$ cm^{-3}. The presence of the TG mode is evident in each case. As B_0 is increased, the H mode dominates near the axis, and this is manifested by the good agreement among the data and the two theoretical curves there. The TG mode was purported to have been seen by Lho et al.[13], but those B-dot data did not show the wings that we could see only with the J-dot probe.

The energy deposition mechanism in helicon discharges is unusual and has been disputed. Electron mass effects giving rise to TG modes had been neglected in early helicon theories; but once included, they yield values of loading resistance agreeing with experiment. Up to now, TG modes had not been observed directly. This work provides evidence for their existence and differs from all previous work on rf discharges by the use of an rf current probe. If these TG modes are indeed relevant to energy deposition, it is predicted[4] that, at the higher magnetic fields used in practice, they would be too localized to be detected but would nonetheless greatly affect the energy absorption.

FIGURE CAPTIONS

1. Diagram of the apparatus.

2. (a) $m = 0$ antenna and Faraday shield. (b) Schematic of J-dot probe.

3. A k–β of Eq. (2) for $f = 11$ MHz, $n = 4 \times 10^{11}$ cm^{-3}, and various fields B_0.

4. Typical radial profiles of $|B_z|$ (•) and $|J_z|$ (O) as (a) calculated and (b, c) measured. In (c) a typical density profile $n(r)$ is also shown, together with the curve used to model it.

5. Magnitudes of $J_z(r)$ and $J_\theta (r)$ obtained by rotating the J-probe 90°, showing the zero-crossing in J_θ. Error bars indicating typical shot-to-shot variation are shown here but omitted in other graphs for clarity.

6. Radial profiles of rf current $|J_z|$ at 30G and various densities (in cm^{-3}) as measured (•), as predicted by theory (––––), and as calculated from simple helicon theory without the TG mode ($- - - -$).

7. Same as Fig. 6 but with varying B_0 at a constant density.

REFERENCES

[1] K.P. Shamrai and V.B. Taranov, Plasma Sources Sci. Technol. **5**, 474 (1996).

[2] F.F. Chen, Plasma Phys. Control. Fusion **33**, 339 (1991).

[3] G.G. Borg and R.W. Boswell, Phys. Plasmas **5**, 564 (1998).

[4] D. Arnush, Phys. Plasmas **7**, 3042 (2000)

[5] D.G. Miljak and F.F. Chen, Plasma Sources Sci. Technol. **7**, 61 (1998).

[6] D.D. Blackwell and F.F. Chen, Plasma Sources Sci. Technol. **6**, 569 (1997).

[7] F.F. Chen and D. Arnush, Phys. Plasmas **4**, 3411 (1997).

[8] D. Arnush and F.F. Chen, Phys. Plasmas **5**, 1239 (1998).

[9] D. D. Blackwell, *thesis*, UCLA (1999).

[10] M. Light and F.F. Chen, Phys. Plasmas **2**, 1084 (1995).

[11] D.G. Miljak and F.F. Chen, Plasma Sources Sci. Technol. **7**, 537 (1998).

[12] F.F. Chen, Phys. Plasmas **8**, 3029 (2001).

[13] T. Lho, N. Hershkowitz, J. Miller, W. Steer, and G.H. Kim, Phys. Plasmas **5**, 3135 (1998).
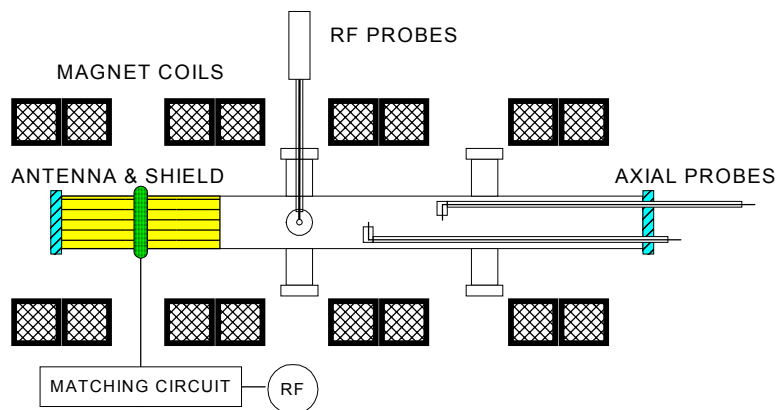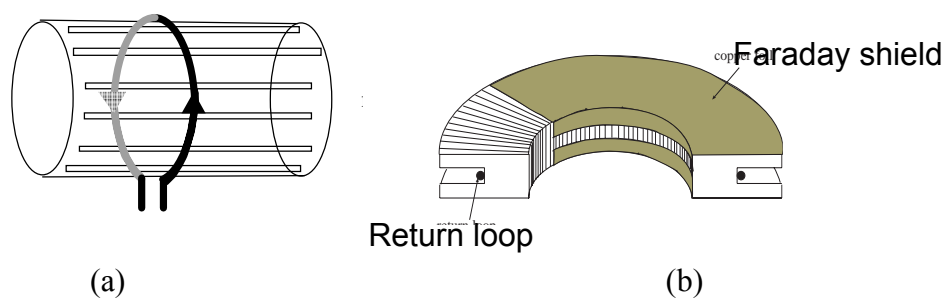
Fig. 1. Diagram of the apparatus.

(a)   (b)

Fig. 2. (a) $m = 0$ antenna and Faraday shield. (b) Schematic of J-dot probe.
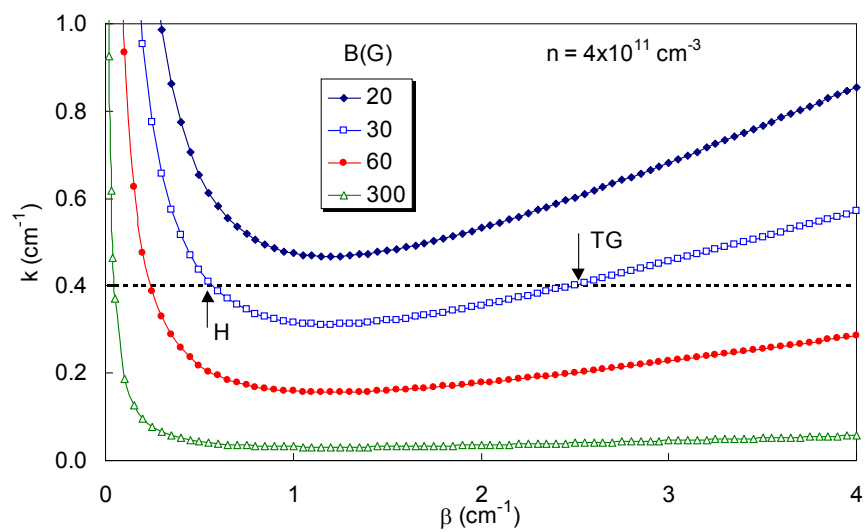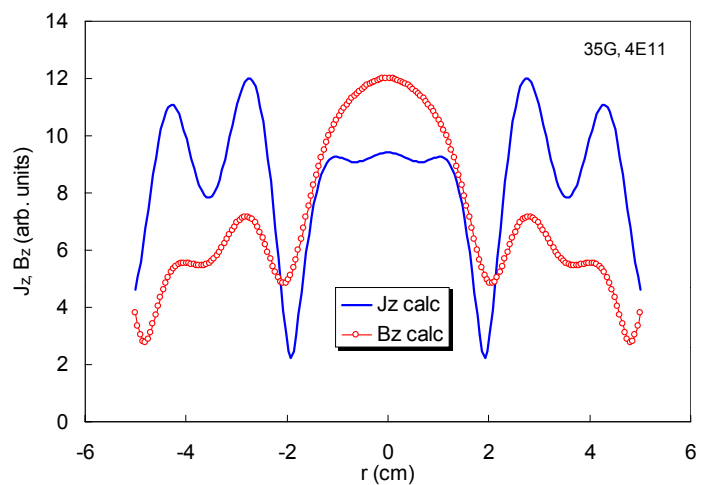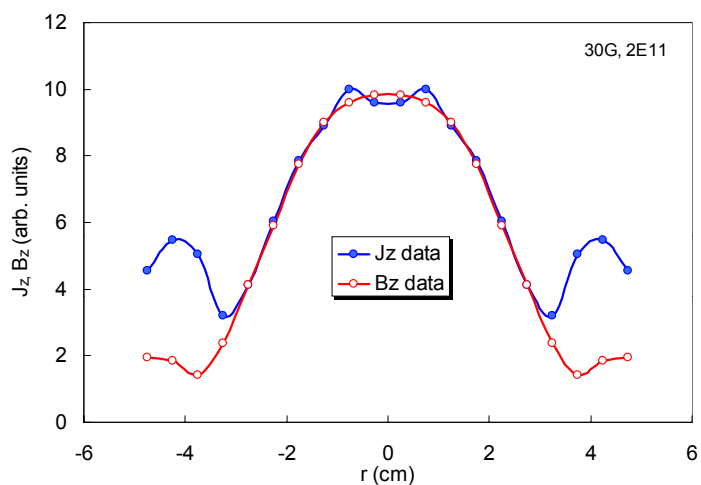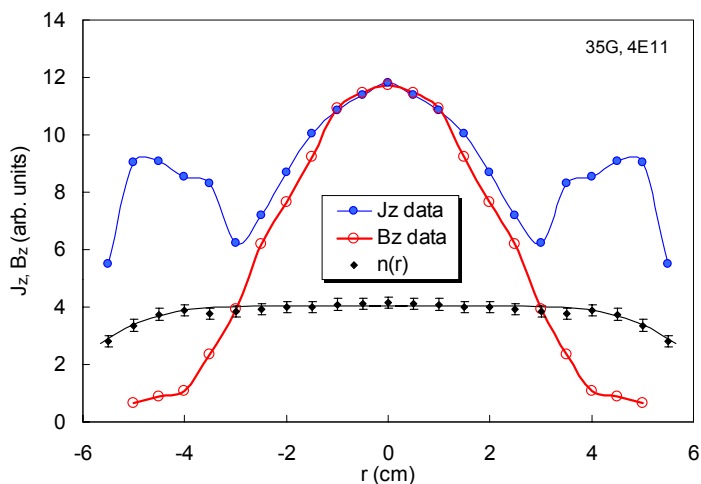

Fig. 3. A k–β of Eq. (2) for $f = 11$ MHz, $n = 4 \times 10^{11}$ cm^{-3}, and various fields B_0.

Fig. 4. Typical radial profiles of $|B_z|$ (●) and $|J_z|$ (○) as (a) calculated and (b, c) measured. In (c) a typical density profile $n(r)$ is also shown, together with the curve used to model it.
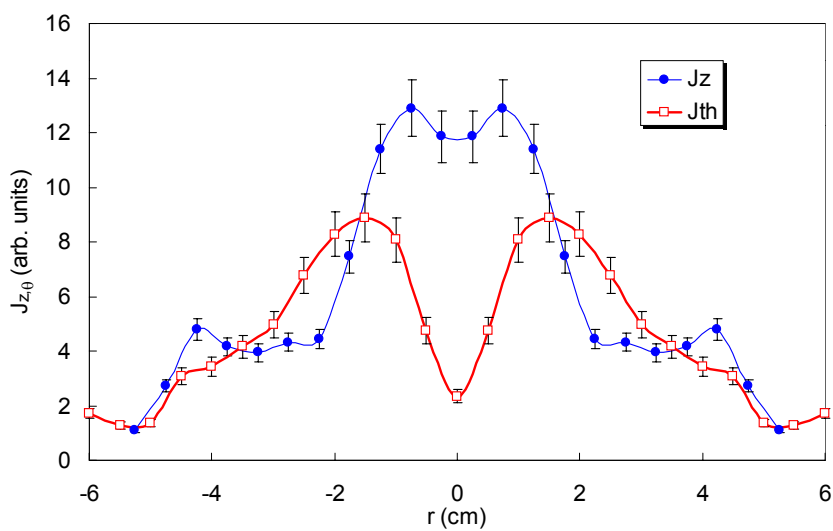
Fig. 5. Magnitudes of $J_z(r)$ and $J_\theta(r)$ obtained by rotating the J-probe 90°, showing the zero-crossing in J_θ. Error bars indicating typical shot-to-shot variation are shown here but omitted in other graphs for clarity.
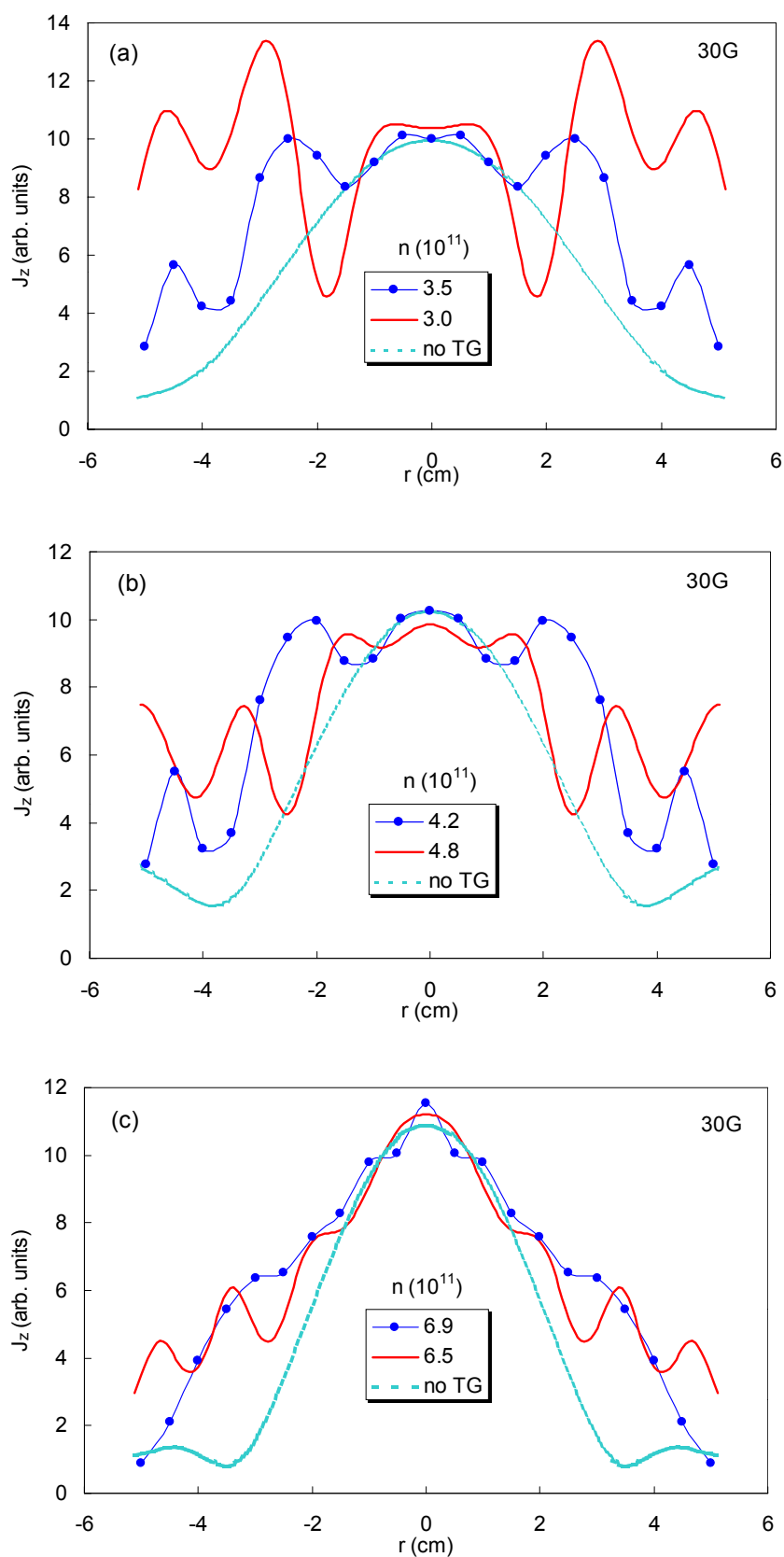
.

Fig. 6. Radial profiles of rf current $|J_z|$ at 30G and various densities (in cm^{-3}) as measured (●), as predicted by theory (———), and as calculated from simple helicon theory without the TG mode ($- - - -$).
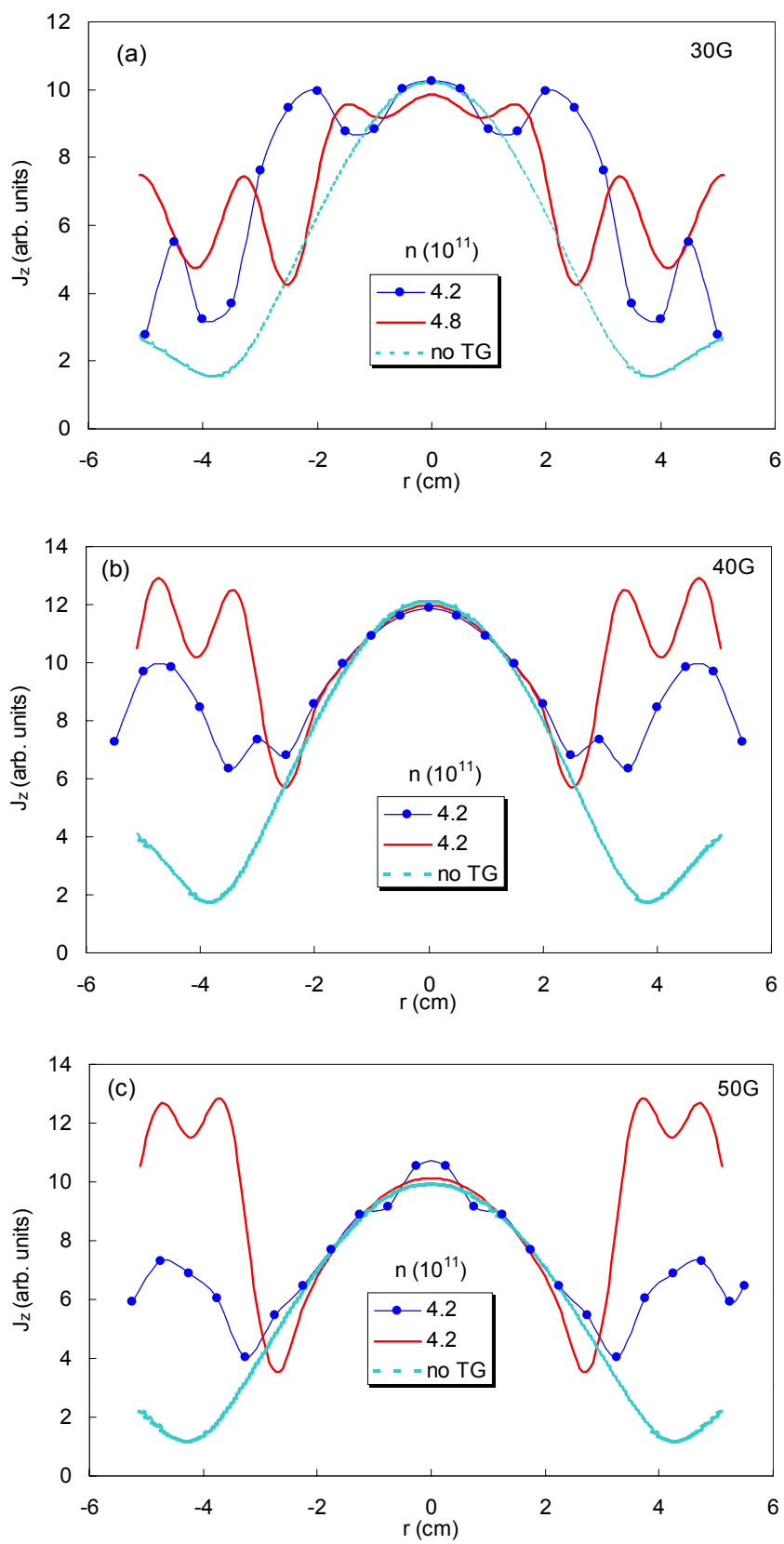
Fig. 7. Same as Fig. 6 but with varying B_0 at a constant density.